

Design and experimental verification of a thin broadband nanocomposite multilayer microwave absorber using genetic algorithm based approach

Ravi Panwar, Vijaya Agarwala, and Dharmendra Singh

Citation: [AIP Conference Proceedings](#) **1620**, 406 (2014); doi: 10.1063/1.4898273

View online: <http://dx.doi.org/10.1063/1.4898273>

View Table of Contents: <http://scitation.aip.org/content/aip/proceeding/aipcp/1620?ver=pdfcov>

Published by the [AIP Publishing](#)

Articles you may be interested in

[Design of an acoustic metamaterial lens using genetic algorithms](#)

J. Acoust. Soc. Am. **132**, 2823 (2012); 10.1121/1.4744942

[Experimental verification of metamaterial based subwavelength microwave absorbers](#)

J. Appl. Phys. **108**, 083113 (2010); 10.1063/1.3493736

[Instrument design and optimization using genetic algorithms](#)

Rev. Sci. Instrum. **77**, 105107 (2006); 10.1063/1.2360987

[Optimal Topology Design of Products Using Genetic Algorithm](#)

AIP Conf. Proc. **712**, 2137 (2004); 10.1063/1.1766851

[High degree of freedom muffler optimization using genetic algorithms: Experimental verification](#)

J. Acoust. Soc. Am. **103**, 3004 (1998); 10.1121/1.421747

Design and Experimental Verification of a Thin Broadband Nanocomposite Multilayer Microwave Absorber using Genetic Algorithm Based Approach

Ravi Panwar^{1,2,a)} Vijaya Agarwala^{1, 3, b)} and Dharmendra Singh^{2, 3, c)}

¹Surface Engineering Laboratory, MMED, ²Microwave Imaging & Space Technology Application Laboratory, ECE

³Nanoelectronics Laboratory, Centre of Excellence: Nanotechnology

Indian Institute of Technology Roorkee

Roorkee-247667, India

^{a)} Corresponding author: rpanwar.iitr@gmail.com

^{b)} agarwala.vijaya@gmail.com

^{c)} dharmfec@gmail.com

Abstract. The bandwidth-thickness tradeoff of single layer microwave wave absorber has become challenge for researchers. This paper presents experimental results of thin broadband multilayer microwave wave absorbing structures using magnetic ceramic based nano-composites for absorption at X-band. A genetic algorithm (GA) based approach has been used to optimize thickness of different material layers and selection of suitable material to ensure minimum reflection. The parameters optimized through genetic algorithm have been simulated through Ansoft High Frequency structural simulator (HFSS) and experimentally verified through Absorption Testing device (ATD). It has been found that the peak value of reflection loss is -24.53 dB for 1.3 mm absorber layer coating thickness, which shows the effectiveness of absorber for various applications..

Keywords: Microwave absorbing material (MAM), Reflection loss (RL), Genetic algorithm (GA), Multi-layering, High frequency structural simulator (HFSS).

PACS: 41.20.Cv, 41.20.Jb, 84.40.Az and 73.63.Bd.

INTRODUCTION

Microwave absorbing material (MAM) has attracted great attention of researchers due to their application in military hardware like aircrafts, missiles, ship and tank etc. to make them invisible to radar wave. It is very difficult for a single material to provide good absorption, minimum absorber layer coating thickness and wide bandwidth together, so now days researchers are using nanocomposite materials having both dielectric and magnetic phase as dielectric phase is necessary to increase the dielectric losses and magnetic phase is essential in order to increase the ability of a material to magnetize[1].

It is very difficult to achieve effective microwave absorption using absorber alone, so current need of research is to utilize the concept of multilayering in order to provide a thin broadband microwave absorber [2]. But

selection of material for different layer as well as preference of layer for multilayered MAM structures is still a challenge for researchers. Yuping et al.[3] recently reported the permissible reflection loss value of -29 dB at 4 GHz by varying the thicknesses of Polyvinyl chloride (PVC) sheet and Polyurethane (PU)/ (carbonyl-iron particle) CIP layer, indicating its effective utilization for low frequency applications. The enhanced microwave absorbing capability of a double-layer microwave absorber (composed of carbonyl iron as the first layer and polycrystalline iron fibers as the second layer) as compared to single layer absorber has been reported by Ding et al.[4]. Yuan et al. [5] have reported a multilayer radar absorbing structure with plasma and MAM and further a stealth point target has been modeled by a four layer absorbing structure. The dielectric inhomogeneous planar layers have been successfully used as optimum microwave absorbers by Amirhosseini et al. [6] in the frequency range of 8–12 GHz and 6–18 GHz.

Multi-layering is a very useful task, as one should have to know the layer thickness, its dielectric and preferences of layers, for these purpose researchers are using different optimization techniques such as particle swarm optimization [7], winning particle optimization [8], central force optimization[9] and genetic algorithm [10] etc. The proper fabrication of optimized multilayer absorber with uniform coating thickness has also become a hurdle in development of MAMs. Various researchers are working to resolve the issue, but still adhesion is a problem, which is very much required for practical applications especially for aircrafts and missiles etc. Software's like HFSS (High frequency Structural simulator), CST (Computer simulation studio) etc. are also be used by various researchers for simulating the various electromagnetic (EM) structures. HFSS being a high performance full-wave EM field simulator may play a significant role for computing the reflection losses of various structures of MAM.

So, in the present study magnetic-ceramic based nanocomposite material has been prepared for fabrication of two layer absorber in the 8.2-12.4 GHz frequency range. The complex permittivity and permeability values are measured in order to compute reflection losses. The optimization of various important parameters for two layer microwave absorber has been carried out using GA based approach with restriction of 2 mm absorber layer coating thickness. The GA optimized values have been simulated with Ansoft HFSS for validation and verification. Further a two layer thin broadband absorber has been fabricated using epoxy based and spray gun coating techniques in order to experimentally validate the results.

MATERIALS AND METHODS

The bottom-up and top-down nanofabrication approaches have been used for developing magnetic ($\text{SrFe}_{12}\text{O}_{19}$) and ceramic (Si-Ti based composite) nanomaterials respectively. Bottom up approach refers to the buildup of a material from the bottom: atom by atom or molecule by molecule. An attempt has been made where bottom up approach is used for development of strontium ferrite nanoparticles by increasing the temperature up to 1100°C.

The $\text{SrFe}_{12}\text{O}_{19}$ particles has been synthesized via sol-gel auto-combustion method which includes the conversion of citrate precursor from sol-to-gel (S-G conversion) followed by gel-to-nanocrystalline powder (G-N Conversion). Stoichiometric amount of analytical grade of ferric nitrate ($\text{Fe}(\text{NO})_3 \cdot 9\text{H}_2\text{O}$), strontium nitrate $\text{Sr}(\text{NO}_3)_2$, citric acid ($\text{C}_6\text{H}_8\text{O}_7 \cdot \text{H}_2\text{O}$) are dissolved in minimum amount of ultrapure de-ionized (DI) water and pH of the solution is maintained up to 7 by using ammonia solution. Then the solution is continuously stirred and heated on a hot plate at constant temperature of 80°C until a brown viscous gel is formed, after sometime dried precursor undergoes a self-ignition (auto-combustion) reaction to form a fine agglomerated brown nanocrystalline powder.

Top down approach refers to break down of bigger particles in to smaller ones. Top-down approach has been employed to reduce micron size (bigger) particles to nano size (smaller) particles. Si-Ti (50:50) based ceramic composite has been reduced to nanometer size powder by milling for 10 h in a high energy planetary ball mill (Model: Retsch, PM 400, Germany) at 200 rpm with 1:5 powder to ball ratio. The materials used for present study are shown in Table 1 and are coded as F, S-T and F+(S-T) respectively throughout the entire study.

The surface morphology of materials has been investigated using carl zeiss scanning electron microscopy, SEM (Model: MA15/EVO18). The samples are prepared by taking 90 wt % material and 10 wt % epoxy resin and cast into a rectangular pellet of thickness 2 mm and cured at 60°C for 1.5 h. The pellets thus prepared were polished to exactly fit into the measuring rectangular waveguide (WR-90). The permittivity and permeability values of developed materials have been measured through Poly Reflection/transmission method in the 8.2-12.4 GHz frequency range at room temperature [11].

TABLE 1. List of Materials used for study

S. No	Material Name	Material Code
1.	SrFe ₁₂ O ₁₉	F
2.	Si-Ti based ceramic powder	S-T
3.	SrFe ₁₂ O ₁₉ + Si-Ti Composite	F+(S-T)

SEM ANALYSIS

The SEM micrographs of sol-gel auto-combustion synthesized F nanoparticles and ball-milled S-T based composites are shown in Figures 1(a) and 1(b) respectively. A SEM image of F shows spherical shape nanoparticles with an average particle size of 30-40 nm as measured by Zeta particle size analyzer (Malvern Zeta sizer ZS90). The SEM image of T-S based composites shows two phase dispersion effect, which plays a significant role in order to achieve excellent microwave absorption as also observed by Kumar et al.[12].

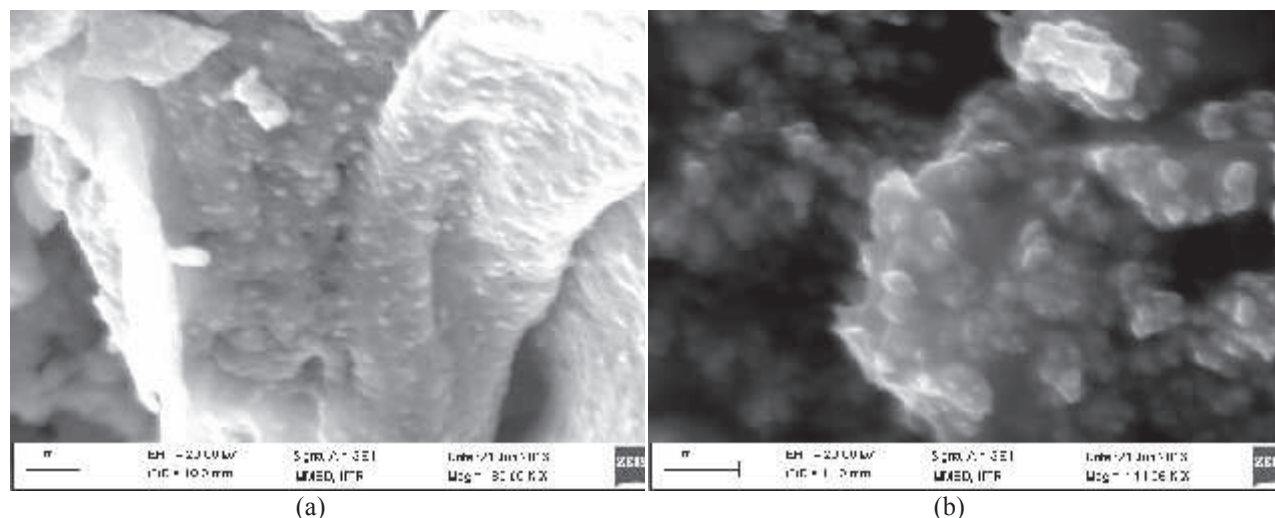


FIGURE 1.SEM micrographs of (a) fine agglomerates of SrFe₁₂O₁₉ nanoparticles and (b) Si-Ti based composite

DIELECTRIC CONSTANT AND REFLECTION LOSS MEASUREMENT

Complex permittivity ($\epsilon_r = \epsilon' - j\epsilon''$) and complex permeability ($\mu_r = \mu' - j\mu''$) represent the dielectric and magnetic properties of MAM. The real parts (ϵ' , μ') accounts for the EM energy storage part, on the other hand, imaginary parts (ϵ'' , μ'') represent EM energy loss part. The RL values for a single layer absorbing material are calculated from the experimentally measured complex permittivity and permeability at given frequency and absorber layer coating thickness using the following equations [12]:

$$Z_{in} = Z_o (\mu_r / \epsilon_r)^{1/2} \tanh \{j(2\pi ft / c)(\mu_r / \epsilon_r)^{1/2}\} \quad (1)$$

Where, f is measurement frequency (for our case 8.2-12.4 GHz), t is the thickness of absorber layer, c is the velocity of light, Z_{in} the characteristic impedance or intrinsic impedance of material, and Z_o is the characteristic impedance or intrinsic impedance of free space.

The frequency dependence of real and imaginary part of complex permittivity measured at X-band frequency range is shown in Figures 2(a) and 2(b). It can be observed that ϵ' , ϵ'' for F is near about constant in nature but for sample S-T and F+(S-T) significant fluctuations have been observed, which may be due to domain wall resonance at low frequency and natural resonance at high frequency[13]. Both ϵ' , ϵ'' has been found to be possess highest values for sample S-T, therefore, presence of S-T in material matrix may be responsible for overall dielectric losses. The peak value of ϵ' , ϵ'' has been noticed as 14.8 at 9.1GHz, and 5.5 at 9.7 GHz respectively.

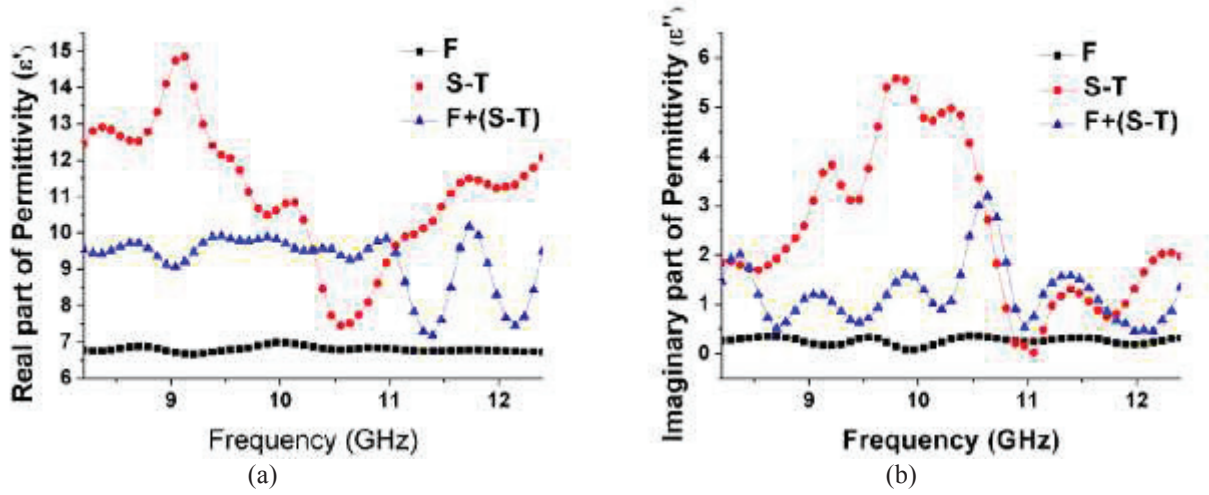


FIGURE 2. Frequency dependence of (a) real and (b) imaginary part of complex permittivity of single layer absorber

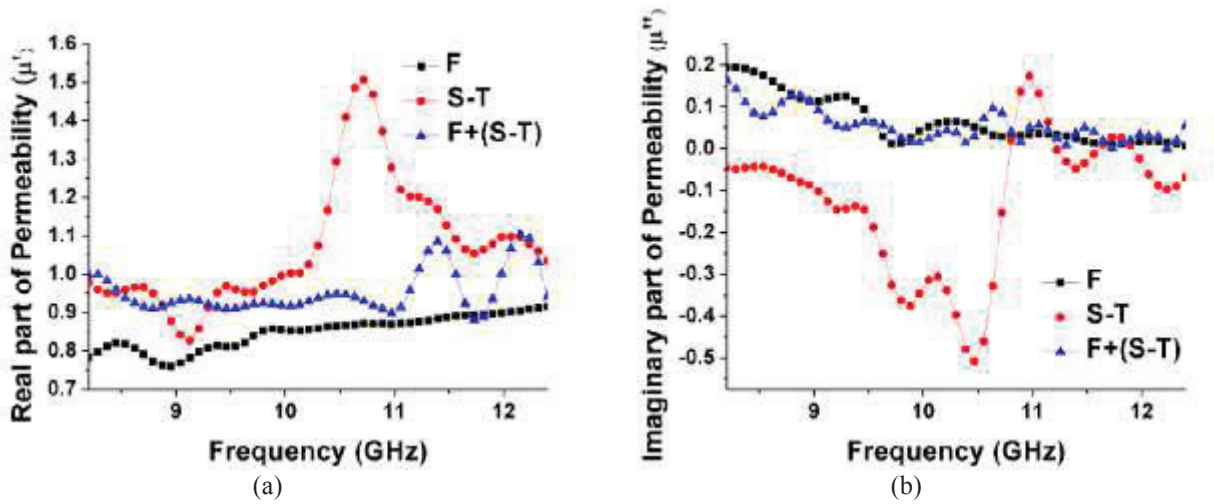


FIGURE 3. Frequency dependence of (a) real and (b) imaginary part of complex permeability of single layer absorber

The frequency dependence of real and imaginary part of complex permeability measured at X-band frequency range is shown in Figure 3(a) and 3(b). The negative value of μ'' for sample S-T may be due to eddy current effect[14]. For the same sample, an inverse trend has been observed among ϵ' , μ' and ϵ'' , μ'' values, similar effect is also observed by Wang et al., such effect may be due to capacitance leading or lagging behind the inductance by an angle of 90° [15]. Reflection loss (RL) is represented:

$$RL(\text{dB}) = -20 \log |(z_{in} - z_o) / (z_{in} + z_o)| \quad (2)$$

The frequency dependent RL characteristics of developed materials have been computed using equation (2) at X-band frequency range and is shown in Figure 4. It clearly appears that the peak RL value for pure F is -10.52 dB at 8.4 GHz for 3.5 mm absorber coating thickness. T has been found to possess a RL of -8.58 dB at 9.7 GHz for 2.5 mm absorber coating thickness. It has been found that addition of S-T composite with F, results in large increase in RL values up to -23.17 dB with corresponding bandwidth of 0.9 GHz ($RL < -10$ dB) for 2.5 mm coating thickness. It has also been noticed that with incorporation of S-T in material matrix peaks are shifting towards higher frequency range, and significant improvement both in RL and bandwidth has been observed. Therefore, F+(S-T) nanocomposite has much more effective microwave absorption as compared to F and S-T, which may be due to presence of both magnetic (F) as well as dielectric phases (S-T) in material matrix, which contributes to overall dielectric and magnetic losses within composite material. The prepared single layer material is found to be provide a good RL but at the cost of increased thickness and narrow bandwidth. Therefore, there is stringent requirement of multi-layering in order to have a thin, broadband microwave absorber.

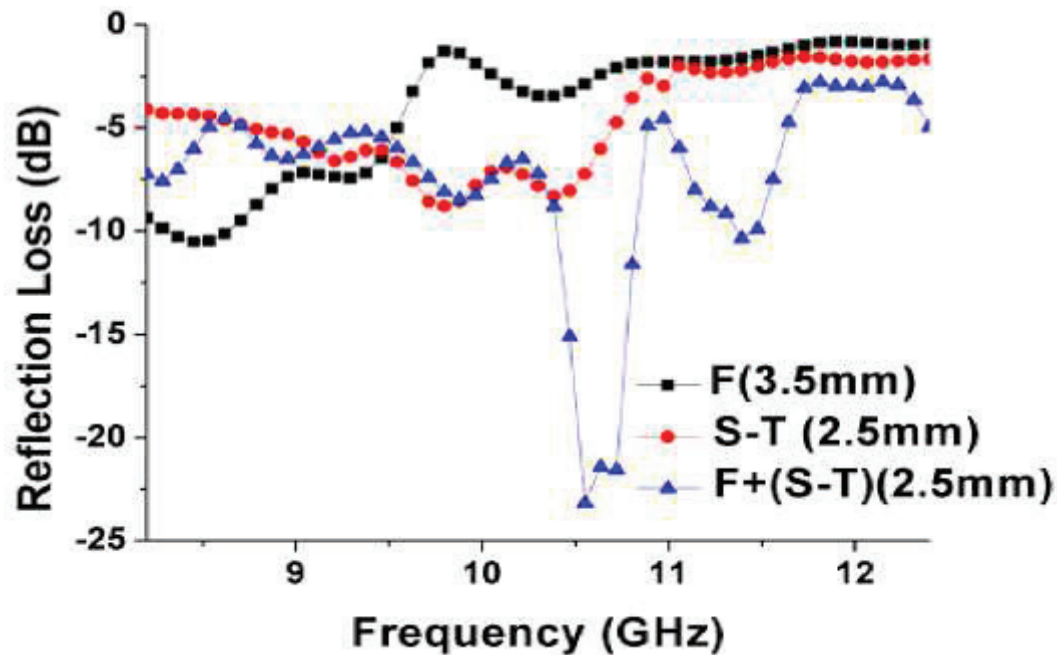


FIGURE 4. Frequency dependence of reflection loss of single layer absorber with corresponding matching thickness

RESULTS AND DISCUSSION

This section consists of details of design as well as fabrication steps of a thin broadband multilayer (two layer) microwave absorber made up of developed magnetic ceramic based nanocomposite material.

Implementation of Two Layer Absorber

The design of multilayer absorber is very difficult, as it requires complicated mathematical equations; therefore, there is need of suitable optimization technique in order to estimate various important parameters such as

the number of material layers, optimal choices of material for each layer, layer preference and its thickness in order to ensure best absorption for a particular frequency band. So here, a two layer absorber has been optimized using GA based approach. GA is basically a search procedure based on mechanics of natural selection and genetics [10].

The fitness function of GA has been developed using transmission line model for analysis of double layer absorber. According to transmission line theory, when an EM wave impinges on an absorber, then it will not be completely absorbed by absorber, some part of it will be transmitted, and some will be reflected and a part of it will be reflected back to the material surface which results in multiple internal reflections due to backscattering of radiation. The reflection coefficient for double layer absorber, where layer 1 is backed with perfect electric conductor and layer 2 is in contact with free space as reported by Truong et al. [16]:

$$\Gamma = \frac{\frac{\sqrt{\frac{\mu_1}{\epsilon_1}} \tanh(\gamma_1 t_1) + \sqrt{\frac{\mu_2}{\epsilon_2}} \tanh(\gamma_2 t_2)}{1 + \sqrt{\frac{\mu_1 \epsilon_2}{\epsilon_1 \mu_2}} \tanh(\gamma_1 t_1) \tanh(\gamma_2 t_2)} - 1}{\frac{\sqrt{\frac{\mu_1}{\epsilon_1}} \tanh(\gamma_1 t_1) + \sqrt{\frac{\mu_2}{\epsilon_2}} \tanh(\gamma_2 t_2)}{1 + \sqrt{\frac{\mu_1 \epsilon_2}{\epsilon_1 \mu_2}} \tanh(\gamma_1 t_1) \tanh(\gamma_2 t_2)} + 1} \quad (3)$$

Where t_1 , ϵ_1 , μ_1 and γ_1 are the thickness, complex permittivity, complex permeability and propagation constant for layer 1, on the other hand, t_2 , ϵ_2 , μ_2 and γ_2 represents the thickness, complex permittivity, complex permeability and propagation constant for layer 2. Here γ is represented as a propagation factor can be expressed as $\gamma = j(2\pi f / c\sqrt{\mu/\epsilon})$.

The measured values of complex permittivity and complex permeability values of developed materials have been used for the analysis of two layer absorber. A thickness restriction of 2 mm has been given to GA in order to provide a thin absorber. The brief description of GA optimization is presented in the form of flow chart as shown in Figure 5. In general, GA optimization starts with defining a fitness function, population, fitness scaling, selection, reproduction, mutation, crossover, migration and hybrid function etc. GA optimization involves four design parameters: two materials (m1 and m2) and their corresponding thickness (t1 and t2) as reported in Table 2. Table 2 shows the best four optimized parameters selected out of 21 combinations of different materials and their thickness. The selections of best combinations have been done on the basis of wide bandwidth and less coating thickness.

TABLE 2. Details of GA optimized design parameters for fabrication of a two layer absorber

S. No	Materials		Thickness		Total Thickness (mm)
	m1	m2	t1 (mm)	t2 (mm)	
1.	S-T	F	1.1	0.2	1.3
2.	S-T	F	1.7	0.2	1.9
3.	S-T	F	1.6	0.2	1.8
4.	S-T	F	1.7	0.3	2.0

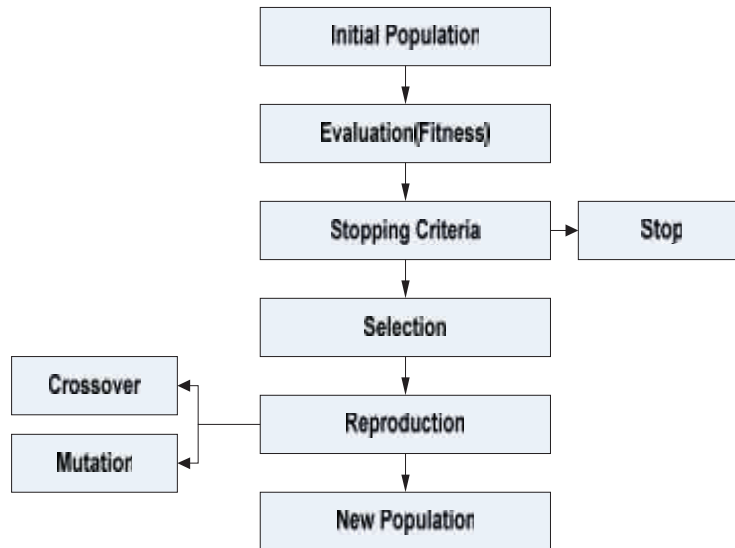


FIGURE 5.Flow chart of Genetic algorithm [10]

Ansoft HFSS Simulation

High Frequency Structural Simulator (HFSS) based on finite element method (FEM), is basically an one of the most useful and powerful tool used for simulation of electromagnetic structures. Here, the main concern is to study the response of microwave absorbing multilayer structures using Ansoft HFSS. The GA optimized parameters as shown in Table 2 have been used to simulate a two layer absorber using Ansoft HFSS for the purpose of validation and verification of optimized results. The HFSS model for a two layer absorber is shown in Figure 6. It has been observed that, strong agreement exist among genetic algorithm based optimized results as well as HFSS simulated results (as shown in Figure 8) which clearly shows the effectiveness of optimization technique.

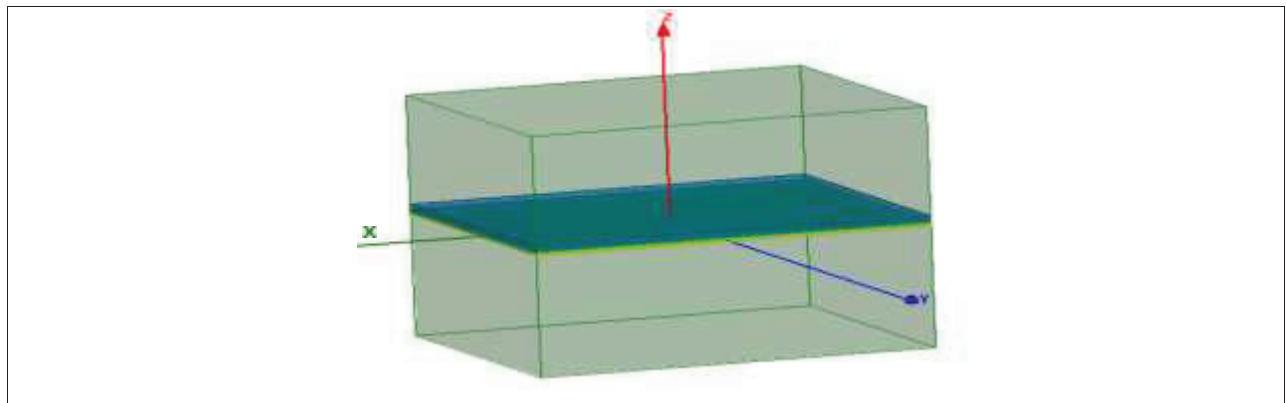


FIGURE 6.Ansoft HFSS Model of a two layer absorber

Fabrication of Two Layer Absorber

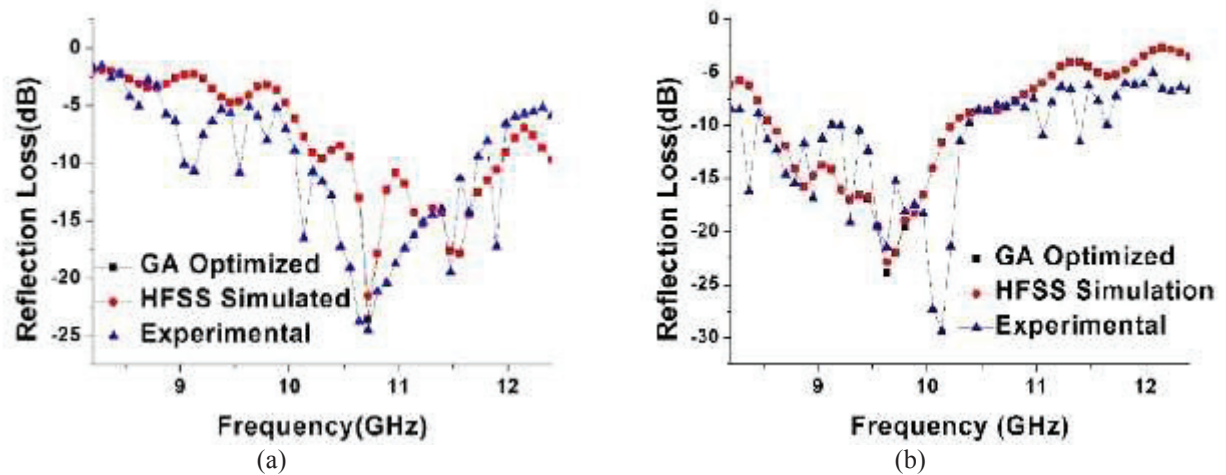
In order to experimentally validate the performance of absorber, a two layer absorber has been fabricated with good adhesion and uniform coating thickness as per optimized parameters from GA using epoxy based and spray gun

coating technique as shown in Figure 7. First of all, S-T based composites with varying thickness have been coated over mild steel sample (94.5×74.2 mm) by employing epoxy based coating as shown in Figure 6(a), and subsequently F has been coated over first layer by spray gun coating technique as shown in Figure 6(b). Further, the heat gun has been used for drying the sample.



FIGURE 7. Fabrication steps for a two layer absorber (a) deposition of first layer of material S-T using epoxy based coating (b) deposition of second layer of material F using spray gun coating technique and (c) fabricated two layer absorber

The ATD [17] which is basically a pyramidal horn antenna has been used for measuring the RL characteristics of absorbers. The frequency dependent RL characteristics of a two layer absorber with varying thickness are shown in Figure 8. The peak RL value for sample 1 has been found to be -24.53 dB at 10.7 GHz with corresponding bandwidth of 2.0 GHz for 1.3 mm absorber coating thickness as shown in Figure 8 (a). Here bandwidth is considered as range of frequencies in which RL is greater than -10 dB, in order to achieve 90% of absorption. A peak RL value of -29.37 dB for sample 2 has been reached at 10.1 GHz for 1.9 mm coating thickness as shown in Figure 8 (b). Further, sample 3 has been found to be providing a peak RL value of -24.46 dB at 9.7 GHz for 1.8 mm absorber coating thickness as shown in Figure 8 (c). Similarly, sample 4 with 2.0 mm coating thickness, has been found to providing a peak RL value of -28.29 dB at 9.2 GHz as shown in Figure 8 (d).



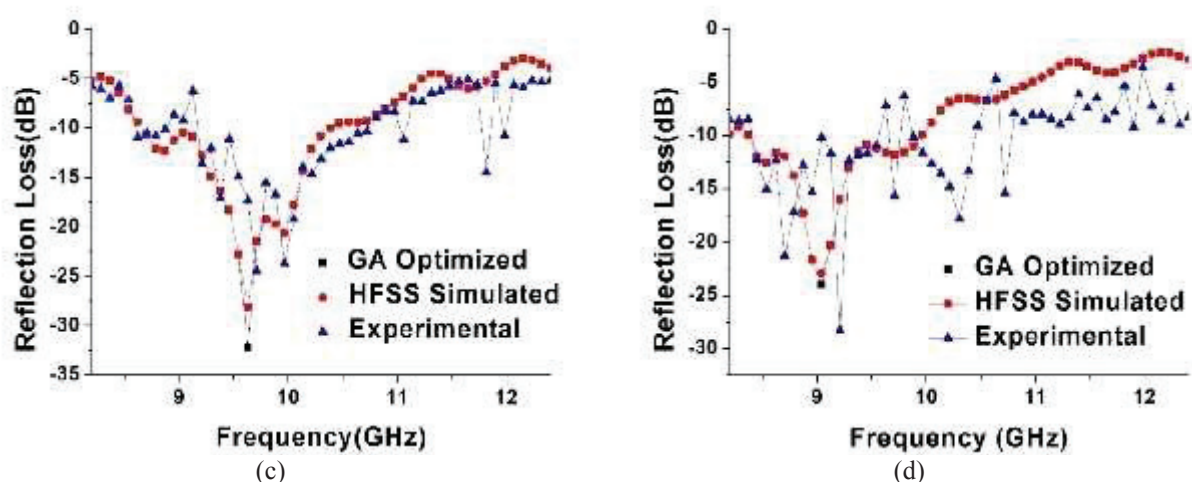


FIGURE 8.Frequency dependent reflection loss characteristic of a two layer absorber with varying thickness (a) sample 1 (1.3 mm) (b) sample 2 (1.9 mm)(c) sample 3 (1.8 mm) and (d) sample 4 (2.0 mm).

TABLE 3. Details of RL characteristics of fabricated two layer thin broadband microwave absorber

S. No.	Sample code	RL (dB)	Frequency (GHz)	Thickness (mm)
1.	Sample 1	-24.53	10.7	1.3
2.	Sample 2	-29.37	10.1	1.9
3.	Sample 3	-24.46	9.7	1.8
4.	Sample 4	-28.29	9.2	2.0

The most interesting thing that emerges from results is that RL strongly depends over absorber layer coating thickness as well as on complex permittivity and permeability values. It can be clearly seen from Table 3 that RL peaks are shifting towards lower frequency with increase of absorber coating thickness. A good agreement has been observed among simulated and experimental results. GA Optimized and HFSS simulated results have been found to be same, but minor fluctuations have been observed in experimental results which may be due to slight thickness variation during coating process.

CONCLUSION

The magnetic ($\text{SrFe}_{12}\text{O}_{19}$)-ceramic (Si-Ti) based nanocomposite materials have been successfully developed by employing top-down and bottom-up nanotechnology based approaches. The experimentally measured complex permittivity and permeability values have been used for computation of reflection loss of single layer as well as for optimization of double layer absorber. The parameters optimized by GA have been verified and validated through Ansoft HFSS, and then experimentally validated by Absorption testing device (ATD). Results proves the strong agreement among simulated and experimental results, which clearly indicates the effectiveness of the microwave absorber. A fabricated two layer absorber has been found to be act as thin broadband absorber with minimum RL value of -24.53 dB with corresponding bandwidth of 2.0 GHz ($\text{RL} < -10$ dB) for 1.3 mm absorber coating thickness. Therefore, developed magnetic-ceramic based nanocomposite materials may be used as a promising microwave absorbing materials especially for defense based applications.

ACKNOWLEDGMENT

The author would like to acknowledge Defence Research & Development Organization (DRDO), New Delhi for providing funding and Ministry of Human Resource Development (MHRD), Government of India for providing fellowship for carrying out this research work.

REFERENCES

1. R. Shang, Y. Zhang, L. Yan, H. Xia, Q. Liu and J. Wang, J. Appl. Phys. **47**, 1-6 (2014).
2. H. Zhang, G. Zeng, Y. Ge, T. Chen and L. Hu, J. Appl. Phys. **105**, 054314 (2009).
3. D. Yuping, W. Guangli, G. Shuchao, L. Shuqing and M. Guojia, Appl. Surf. Sci. **258**, 5746- 5752 (2012).
4. Q. Ding, M. Zhang, C. Zhang and T. Qian, J. Magn. Magn. Mater. **331**, 77-81 (2013).
5. C. Yuan, Z. Zhou, J. Zhang, X. Xiang, Y. Feng and H. Sun, IEEE Trans. Plasma Sci., **39**, 1768-1775 (2011).
6. M. Amirhosseini, IET Microw. Ant. Propag. **4**, 2228-2233 (2010).
7. S. Chamaani, S. Mirtaheri and M. Shooredeli, Int. J. Electron. Commun. **62**, 549-556 (2008).
8. D. Micheli, C. Apollo, R. Pastore, D. Barbera, R. Morles, M. Marchetti, G. Gradoni, V. Primiani and F. Moglie, IEEE Trans. Electromag. Comp. **54**, 60-69 (2012).
9. M. J. Asi and N. I. Dib, Prog. Electromag. Res. B **26**, 101-113 (2010).
10. S. Zouhdi, A. Sihvola and A.P Vinogradov, *Metamaterials and Plasmonics, Fundamentals, Modelling, Applications*(Springer, Netherlands, 2009) pp.153-164.
11. A. Kumar, V. Agarwala and D. Singh, Prog. Electromag. Res. M **29**, 223-236 (2013).
12. A. Kumar, V. Agarwala and D. Singh, Ceram. Int. **40**, 1797-1806 (2014).
13. A. Oikonomou, T. Giannakopoulou and G. Litsardakis, J. Magn. Magn. Mater. **316**, 827-830 (2007).
14. Y. Wang, L. Wang and H. Wu, Materials **6**, 1520-1529 (2013).
15. H. Wu, L. Wang, Y. Wang, S. Guo and Z. Shen, J. Alloys Compd. **525**, 82-86 (2012).
16. V.T Truong, S.Z Riddell and R.F Muscat, J. Mat. Sci. **33**, 4971-4976 (1998).
17. M.R. Meshram, N. K. Agrawal, B. Sinha and P.S. Misra, J. Magn. Magn. Mater. **271**, 207-214 (2004).